THREE-DIMENSIONAL PHOTOELASTIC ANALYSIS OF THE LOAD DISTRIBUTION IN A SUCKER-ROD JOINT

By

Monroe Upton Ayres, Jr.

Bachelor of Science

Oklahoma State University

Stillwater, Oklahoma

1960

Submitted to the faculty of the Graduate School of
the Oklahoma State University
in partial fulfillment of the requirements
for the degree of
MASTER OF SCIENCE
May, 1961

THREE-DIMENSIONAL PHOTOELASTIC ANALYSIS

OF THE LOAD DISTRIBUTION

IN A SUCKER-ROD JOINT

Thesis Approved:

W. H. Easton

Thesis Adviser

Rollo E Uenn

Dean of the Graduate School

PREFACE

The purpose of this experiment was to determine the effectiveness of an undercut pin design in reducing stress concentration in a sucker-rod joint. The undercut pin designed by The W. C. Norris Manufacturing Company in Tulsa, Oklahoma, can be manufactured from present sucker-rod forgings.

A three-dimensional photoelastic investigation was conducted to compare an undercut pin with a standard API pin. The two pins were used in one joint in order to obtain similar loading conditions on each pin.

I express my appreciation to Prof. W. H. Easton for his guidance while conducting the research and writing this thesis. I am grateful to Dr. J. H. Boggs for his advice and encouragement throughout my graduate studies. Recognition is due Vice-Dean R. E. Venn for reviewing this thesis. I wish to thank Mr. J. E. Cox for his assistance with the project. I am grateful to my wife, Marilyn, for typing this thesis. Gratitude is expressed to my parents, Mr. and Mrs. M. U. Ayres, for their contributions to my education.

TABLE OF CONTENTS

LIST OF TABLES

LIST OF FIGURES

LIST OF PLATES

SYMBOLS

A_c	Area of coupling (in^2)
A_p	Area of pin (in^2)
d_c	Friction diameter of the coupling (in)
d_m	Mean diameter of the threads (in)
E_p	Modulus of Elasticity for the pin (psi)
E_c	Modulus of Elasticity for the coupling (psi)
E_{77}	Modulus of Elasticity of Hysol 6000-OP at 77 ^oF (480,000 psi)
E_{270}	Modulus of Elasticity of Hysol 6000-OP at 270 ^oF (2,190 psi)
F	Tensile preload force (lb)
^oF	Temperature, degrees Fahrenheit
F_{77}	Preload force in the coupling at room temperature (lb)
F_{270}	Portion of the external force in the coupling at 270 ^oF (lb)
f	Coefficient of friction for the threads
f_c	Coefficient of friction for the coupling
G	Model fringe value (psi/fringe)
g	Material fringe value (psi/fringe/inch)
k	Maximum fillet stress/Average stress
K_c	Equivalent spring constant for the coupling (lb/in)
K_p	Equivalent spring constant for the pin (lb/in)
L_c	Characteristic length of the coupling (in)
L_p	Characteristic length of the pin (in)
l	Lead of the threads (in)

N	Fringe order
P	Principal stress (psi)
Q	Principal stress (psi)
t	Thickness of the center slice of the model (in)
W	External load (lb)
W_c	Portion of the external load carried by the coupling (lb)
W_p	Portion of the external load carried by the pin (lb)
1G	First green fringe (This is the first order fringe)
1Y	First Yellow fringe (1/3 of the first green)
1R	First red fringe (2/3 of the first green)
β_n	Angle between the axis of the thread and the normal to the surface at the point of contact on the thread
Δ	Deflection (in)
Δ_c	Deflection of the coupling (in)
Δ_p	Deflection of the pin (in)
Δ_{77}	Deflection due to the preloading at 77 ^{o}F (in)
Δ_{270}	Deflection due to the external load at 270 ^{o}F (in)

CHAPTER I

INTRODUCTION

For a number of years, the load distribution in the sucker-rod joint was of minor importance. The sucker-rod strings operating in shallow wells did not experience large loads. Modern machinery is capable of drilling much deeper wells. The sucker-rod strings operating in these wells experience larger loads. These loads fluctuate and may produce fatigue failures. Approximately ninety per cent of all fatigue failures in sucker-rod strings occur at the first full thread in the pin joint. (1).

These failures are the result of load concentration at the first thread in the standard API pin. Satisfactory operation of sucker-rod strings in deep wells requires that the sucker-rod joints be designed to transmit larger loads with a minimum amount of load concentration at any point in the pins.

Several methods exist for distributing the load in a threaded connection. (2). The American Petroleum Institute Standardization Committee for Sucker-Rod Design is considering adopting the new undercut pin design as a means of reducing pin failures due to load concentration at the first full thread. In order to determine the effectiveness of the undercut pin design, a joint was made and tested using one undercut pin and one API standard pin. The results of this comparison are presented in this thesis.

CHAPTER II

SUCKER-ROD FAILURES

Sucker-rod failures are of three basic types. One type failure may occur from wear as the pin joint rubs the inside of the well casing. A second type may result from faulty workmanship or defective material. A third type may result from fatigue failure of the sucker rod. Approximately ninety-nine per cent of all sucker-rod failures are fatigue failures. (3).

The fatigue failure of the sucker rod may occur in four principal locations--the body, the wrench flats, the threaded pin, or the threaded coupling. The body of the sucker rod is the weakest part of the rod structurally. Therefore, it is desirable that the eventual failure, if one occurs, should be in the body of the rod--two to three inches away from the pin. This latter position is most vulnerable even in a perfect rod because variation of the cross section of the rod results in stress concentration at that point. (3). Breaks that occur at other points in the body would be the result of imperfections in the material. These imperfections may be due to improper handling of the rods, resulting in a notch or scratch on the rod surface with stress concentration at that point. Stress concentration may also be produced by concentrated corrosion of the material on the rod surface.

The wrench-flat portion of the rod is of greater cross-sectional area than the other portions of the rod. Any failures in this area can

be traced to improper workmanship or defective material. This type of failure is very rare. (3).

Pin breaks are fatigue failures originating at a point of high-stress concentration at the threads. By limiting the range stress that exists in the pin under a repeated load, the effect of the stress concentration on the threads can be reduced. The range stress can be reduced by increasing the make-up torque on the joint.

If sufficient preload is not induced in the pin to prevent the contact faces from separating under load, the pin, which is necessarily subjected to stress concentration, will not only be subjected to a high range of stress but will also be subjected to bending. Bending may occur when the shoulder face and the coupling face separate under load. Bending can be eliminated by producing sufficient preloading of the joint.

Fatigue failures may also occur in the couplings. The couplings are subjected to repeated loads. Coupling breaks primarily originate at the inside surface. This is a result of the stress concentration at the threads and the corrosive action from fluid that might seep into the joints. Failures that originate at the outside surface of the coupling may be due to hammer blows, scratches, or notches on the hardened surface.

In general, the endurance life of a metal part subjected to fatigue can be improved by: (1) lowering the maximum stress by increasing the cross-sectional area, (2) decreasing the effect of corrosion by the use of an inhibitor-type grease, (3) decreasing the range stress by initial preloading, and (4) eliminating stress concentration, such as sharp notches. (1).

CHAPTER III

EXPERIMENTAL APPARATUS

The three-dimensional investigation of the sucker-rod joint utilized the equipment as explained in this chapter. The loading frame and the oven were used to freeze the stresses into the model. The photoelastic equipment was used to analyze the results.

The Sucker-Rod Joint

The sucker-rod joint used in this experiment was composed of one API standard pin and one undercut pin. The dimensions of the pins and the coupling simulated those in a three-quarter-inch sucker-rod string. The sucker-rod joint components were made of Hysol 6000-0P at the Research and Development Laboratory of Oklahoma State University. Hysol 6000-0P is a new photoelastic material manufactured specifically for three-dimensional investigations. (4). The details of the API standard pin, the undercut pin, and the coupling are shown in Plate I and in Figures 1, 2, and 3 respectively.

The undercut pin was designed to accomplish three things. First, and most important, the design was to reduce the stress concentration at the first full thread in the pin. Second, the long, slender neck has a lower spring constant; thus, the undercut pin will elongate more due to tightening than the standard API pin. This additional elongation tends to offset relaxation which occurs under operation and to assist in

PIATE I

SUCKER-ROD JOINT COMPONENTS

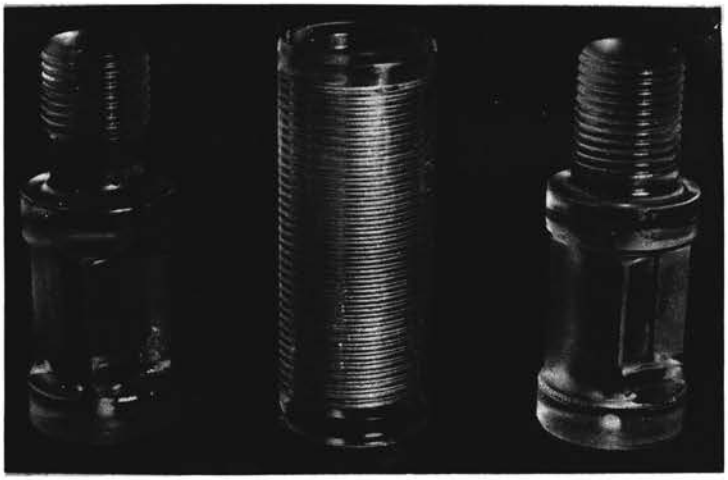

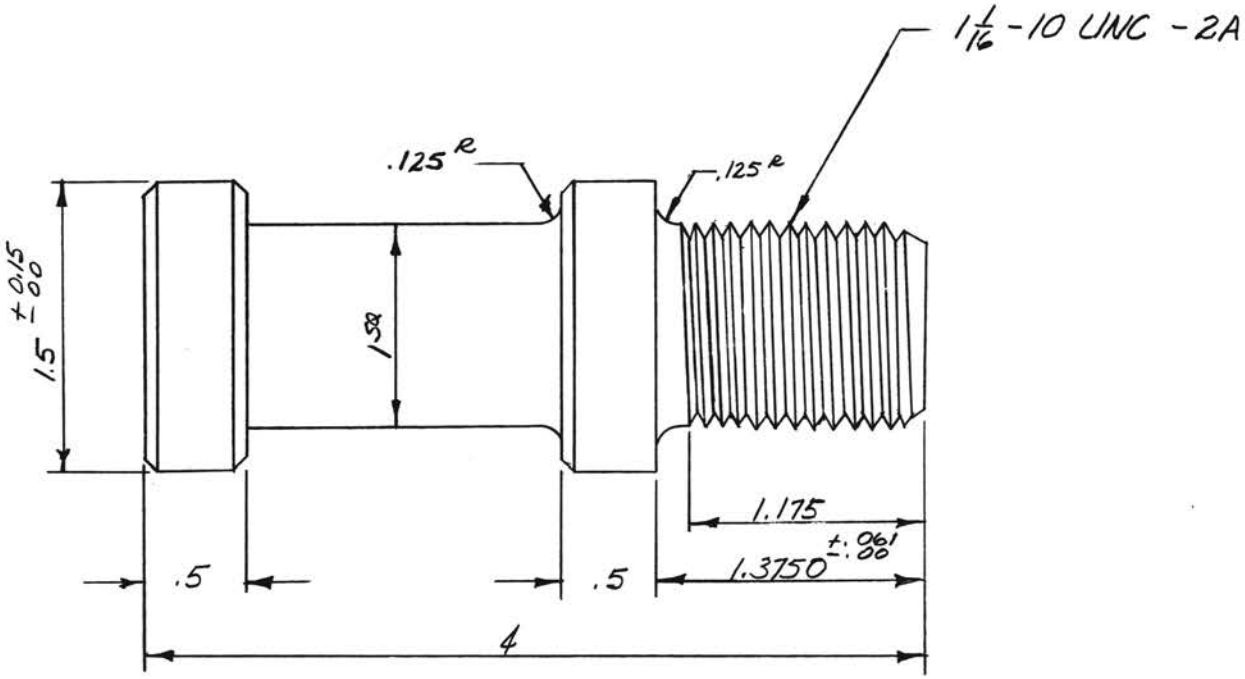

Figure 1. Standard API Sucker-Rod Pin

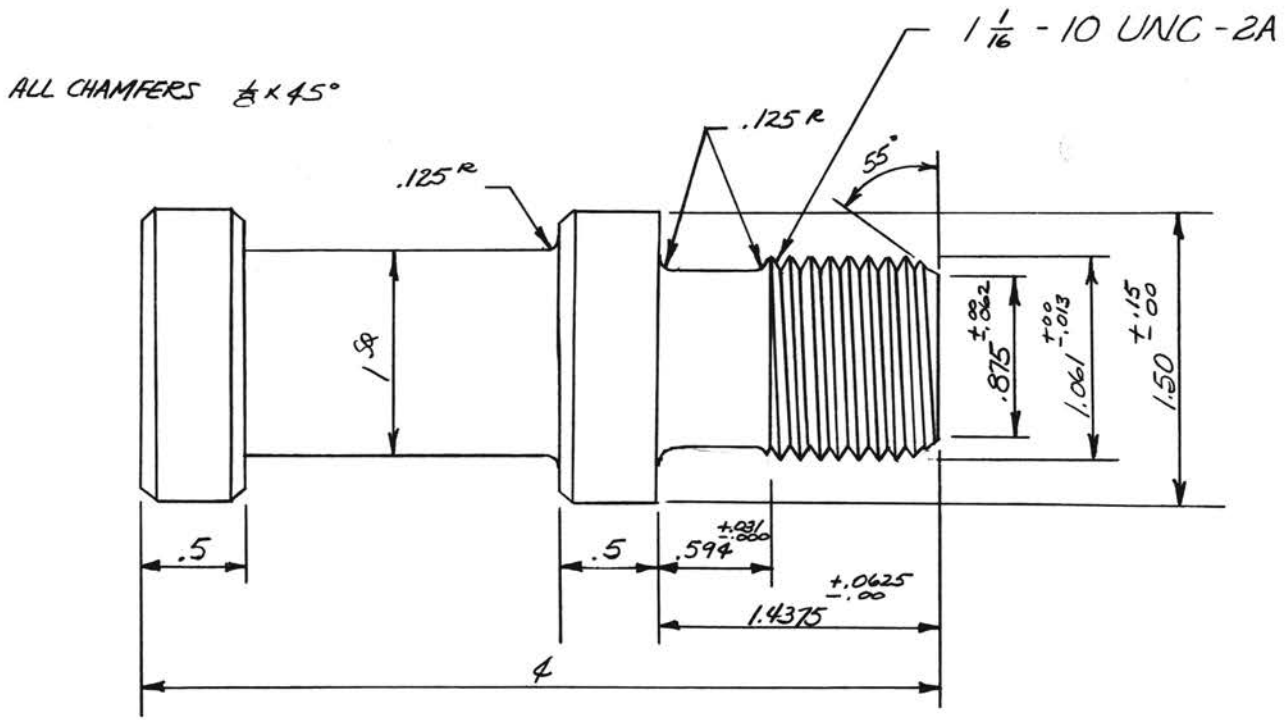

Figure 2. Undercut Sucker-Rod Pin

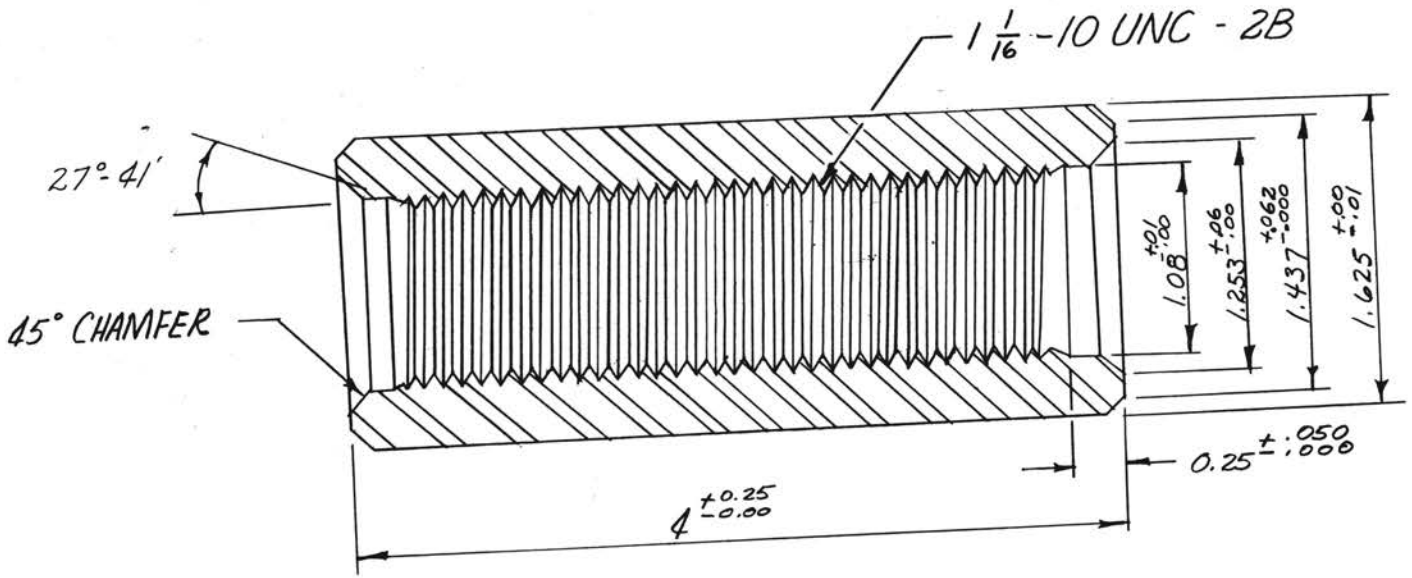

Figure 3. Standard API Sucker-Rod Coupling

maintaining a tight joint. Third, if bending should produce similar deflections in the pin joints, the tensile stresses on the extreme fiber of the undercut pin will be appreciably lower than on the API standard pin. The lower value of stress reduces the chances of fatigue. Of course, bending does not occur if the bases do not separate; but occasionally the bases do separate. The undercut pin design allows the operator greater latitude in the make-up torque applied to the joint. (5).

The Annealing Oven

The annealing oven was designed and built by Max M. Spencer to obtain a constant cooling rate of approximately 2 ^{o}F per hour. The oven was controlled by a variac which was used to decrease the voltage applied to the heating elements as the oven temperature decreased. The oven and its control equipment are shown in Plate II. The approximate temperature of the model was measured by a type J thermocouple secured between two one-half-inch slices of Hysol 6000-OP.

The Stress Freezing Oven and the Loading Frame

The Precision Scientific oven shown in Plate III was used for the stress-freezing operation. The temperature in the oven was controlled by a bi-metallic switch located at the top of the oven. The oven was heated to a temperature of 270 ^{o}F and held at this temperature until the thermocouple located in the center of the Hysol 6000-OP block indicated the model was at a uniform temperature of 270 ^{o}F. The oven was cooled at the rate of approximately 2 ^{o}F per hour by the mechanism attached to the bi-metallic switch as shown in Plate III.

PIATE II

ANNEALING OVEN AND CONTROLS

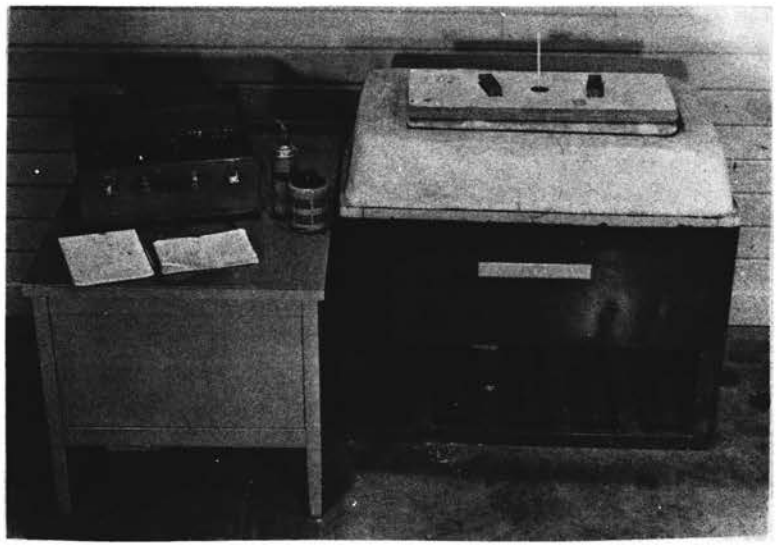

PLATE III

STRESS-FREEZING OVEN, CONTROLS, AND LOADING FRAME

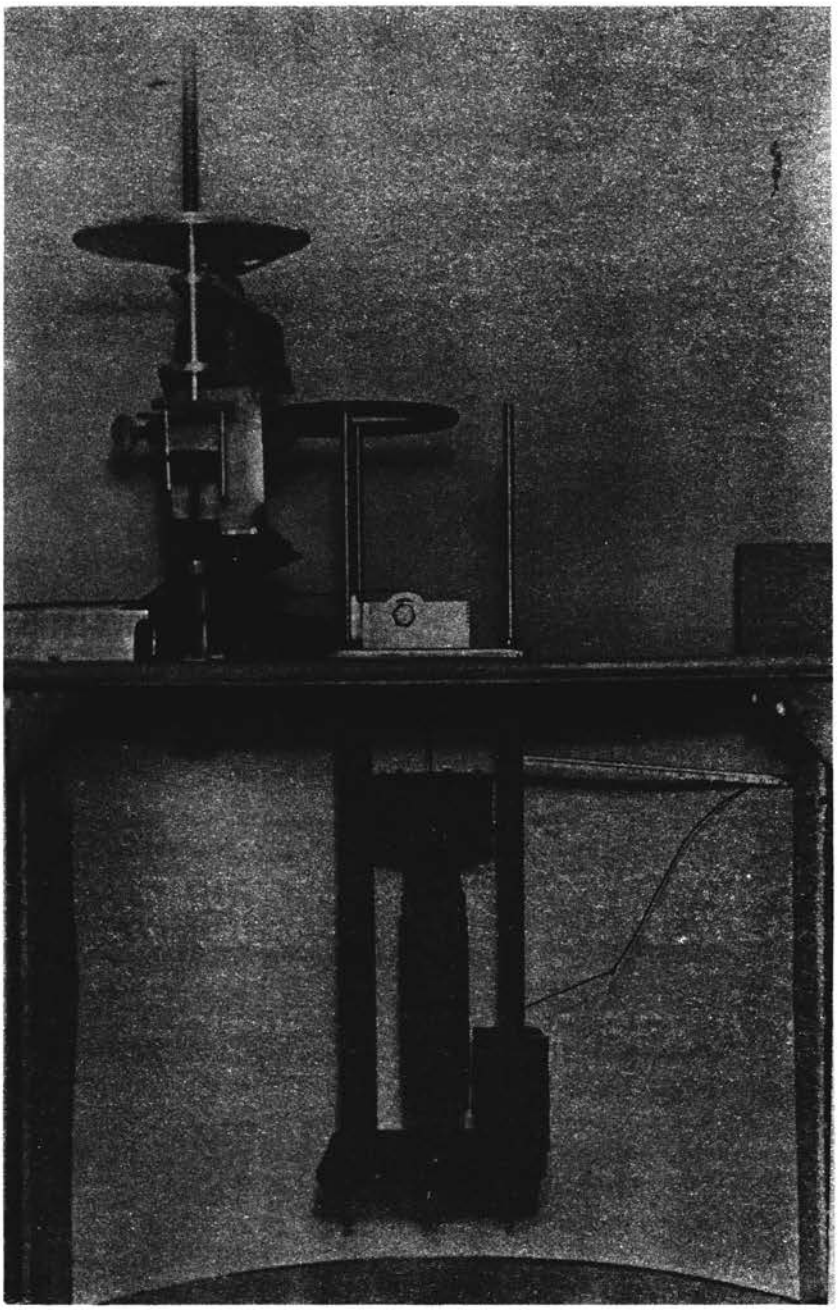

The loading frame shown in Figures 9a and 9b in Appendix E and Plate III was supported from a one-sixteenth-inch steel plate built into the top of the oven. The components of the loading frame were designed rigid enough so that there would be no significant deflection upon application of the load. By eliminating any deflections in the loading frame, a pure axial load could be applied to the model.

The external load is applied by a cable passing through the top of the oven. By loading the model from the top, the effect of the weight of the loading system can be canceled and the external load may be accurately determined.

The Photoelastic Equipment

The polariscope shown in Plate IV was a standard transmission type with a 300-watt projection lamp. Monochromatic light was obtained by inserting a narrow band 5461 line interference filter in front of the camera lens.

Circularly polarized light was used for viewing the fringe patterns; therefore, the quarter-wave plates were placed in the optical path. The fringe pattern was projected onto the ground-glass plate of the camera.

Photographs produced a permanent record of the fringe pattern in the model. The method of photographing the fringe pattern is described in Appendix A.

PLATE IV

POLARISCOPE ARRANGEMENT FOR OBTAINING FRINGE PATTERN

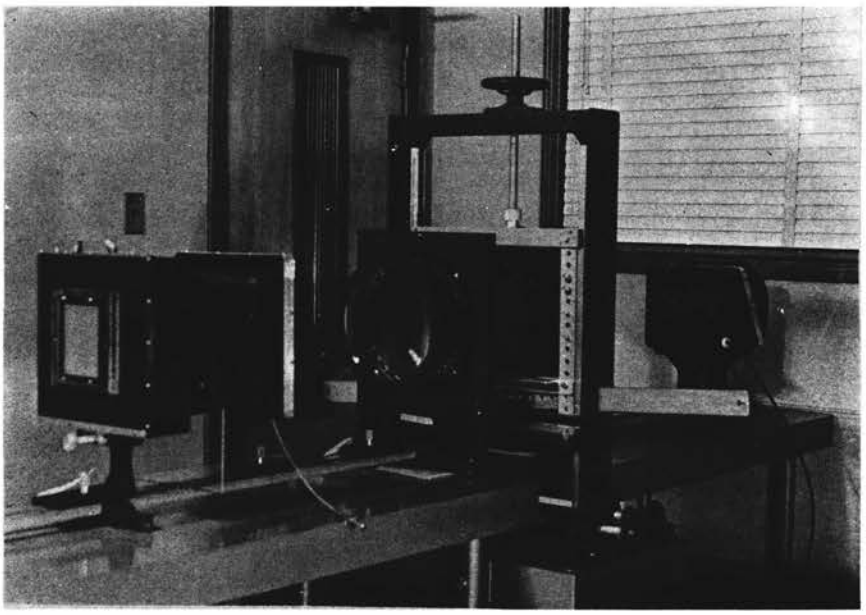

CHAPTER IV

EXPERIMENTAL PROCEDURE

The most satisfactory operation of a sucker-rod joint is obtained when the surfaces of the coupling and the shoulder of the pin remain in contact. It was desirable for this condition to exist in the model when the load was applied. To determine the relationship between the external load and the torque required for preloading, an equation was derived in the following manner.

Derivation

The torque required to preload the threaded joint with a tensile force F may be expressed as

$$T = \frac{Fd_m}{2}\left(\frac{l + \pi d_m f \operatorname{Sec}\beta_n}{\pi d_m - f l \operatorname{Sec}\beta_n}\right) + \left(\frac{F f_c d_c}{2}\right) \qquad (6)$$

where

T - Torque (in-lb)

F - Tensile preload force (lb)

d_m - Mean diameter of the threads (in.)

l - Lead of the threads (in.)

f - Coefficient of friction for the threads

β_n - Angle between the axis of the thread and the normal to the surface at the point of contact on the thread

f_c - Coefficient of friction for the coupling

d_c - Mean diameter of the coupling.

Using the dimensions of the model and a coefficient of friction for Hysol 6000-OP of 0.25, the torque required to preload the model was

$$T = 0.328\ F\ .$$

In order to simulate the actual conditions that exist in the steel rod, it was necessary that contact be maintained between the coupling and the shoulder of the pin after the load was applied. The distribution of the external load to each member is determined by considering the system as two springs. The outside spring is the coupling, and the inside spring is the pin. After the joint is tightened and before the load is applied, the external spring is loaded in compression and the internal spring is loaded in tension.

When the load is applied, both springs must deflect an equal amount if contact is to be maintained. Considering that

$$W = \triangle K$$

and

$$\triangle_c = \triangle_p\ ,$$

it follows that

$$\frac{W_c}{K_c} = \frac{W_p}{K_p}\ .$$

When contact does exist, the application of the external load results in an increase of the tensile force in the shank of the pin and a decrease of the compressive force in a similar length of the coupling, or

$$W = W_c + W_p\ .$$

By substitution

$$\frac{W - W_p}{K_c} = \frac{W_p}{K_p}\ ,$$

or the portion of the external load carried by the coupling and the pin is

$$W_p = \left(\frac{K_p}{K_p + K_c}\right) W$$

and $$W_c = \left(\frac{K_c}{K_p + K_c}\right) W \ .$$

The spring constant K for the coupling and pin may be expressed as

$$K = \frac{AE}{L}$$

since $$E_p = E_c \text{ and } L_p = L_c$$

$$W_p = \left(\frac{A_p}{A_p + A_c}\right) W$$

$$W_c = \left(\frac{A_c}{A_p + A_c}\right) W \ .$$

For the undercut model, the portion of the external load carried by the coupling and the pin is

$$W_p = 0.358\ W$$

$$W_c = 0.641\ W$$

Therefore it is evident that the force on the inner spring is not equal to the external load that is applied. Or, in terms of a sucker-rod joint, the stress in the pin is a function not only of the load on the sucker-rod string, but also of the respective cross-sectional areas of the pin and coupling.

To simulate the condition that exists in a sucker-rod joint, the contact faces in the Hysol 6000-OP model should not separate under the applied load. Due to the change in the modulus of elasticity when the material is heated to 270 °F, the internal force F due to preloading will change; however, the deflections in the model will remain the same. Therefore, the deflection in the coupling produced by the load at 270 °F must be less than the deflection in the coupling due to preloading at 77 °F if the shoulder of the pin and the coupling are to remain in

contact. The deflection in the coupling may be expressed as

$$\Delta = \frac{FL}{AE} .$$

Since $$\Delta_{270} < \Delta_{77} ,$$

it follows that $$\left(\frac{FL}{AE}\right)_{270} < \left(\frac{FL}{AE}\right)_{77}$$

or $$F_{270} < \left(\frac{AE}{L}\right)_{270} \left(\frac{L}{AE}\right)_{77} \left(F_{77}\right)$$

where F_{270} is a portion of the external load acting through the coupling and F_{77} is the initial preload in the coupling.

The portion of the external load carried by the coupling is

$$F_{270} = \left(\frac{A_c}{A_c + A_p}\right) W .$$

The initial preload force in the coupling was found to be

$$F = \frac{T}{0.328} .$$

Therefore the external load W may be determined by

$$W < \left(\frac{A_c + A_p}{A_c}\right) \left(\frac{AE}{L}\right)_{270} \left(\frac{L}{AE}\right)_{77} \left(\frac{T}{0.328}\right)$$

where

W = External load (lb)

A_c = Cross-sectional area of the coupling (in^2)

A_p = Cross-sectional area of the pin (in^2)

E_{270} = Modulus of Elasticity at 270 °F (psi)

E_{77} = Modulus of Elasticity at 77 °F (psi)

L_{270} = Reference length (in.)

L_{77} = Reference length (in.)

T = Torque (in-lb).

Based on the dimensions of the undercut pin and the coupling, the tightening torque required for different external loads may be expressed as

$$W = 0.0218\ T.$$

These values are shown in Table I.

TABLE I

MAKE-UP TORQUE FOR DIFFERENT EXTERNAL LOADS

Weight (lb)	Torque (in-lb)
1	45.9
2	91.8
3	137.7
4	183.6
5	224.5
6	275.4
7	321.3
8	367.2
9	413.1
10	459
11	505
12	551
13	697
14	743
15	789

The external load could be chosen depending on the maximum make-up torque that the model could withstand and not fail. The make-up torque applied to the model was 367 in-lb. The external load applied to the model was seven pounds. A load of one pound less than the maximum was used in order to insure that separation would not occur.

Annealing

The two sucker-rod pins and the coupling were placed in a halowax bath in order to determine if any machining stresses were present. The halowax bath was mixed so that the index of refraction of the solution was equal to the index of refraction of Hysol 6000-OP. The fringes shown in Plate V indicated that machining stresses were present in the model. Therefore, it was necessary to anneal the model in order to relieve the machining stresses.

The annealing process was conducted in the oven designed and built by Max M. Spencer. (4). The oven was heated by increasing the input voltage until equilibrium was maintained at 280 ^{o}F. The oven was opened and the model was placed on a sheet of asbestos board in such a manner as to prevent any deflections or distortions in the model. The model was protected from direct radiation or conduction from the coils by the use of the cavity liners in the oven. The temperature of the oven was maintained at 280 ^{o}F for twelve hours. Twelve hours was a sufficient amount of time for the entire model to reach thermal equilibrium at a temperature of 280 ^{o}F.

The voltage was reduced as shown in Table VIII in order that the temperature of the model would decrease at a constant rate. The cooling

PLATE V

API STANDARD PIN BEFORE ANNEALING

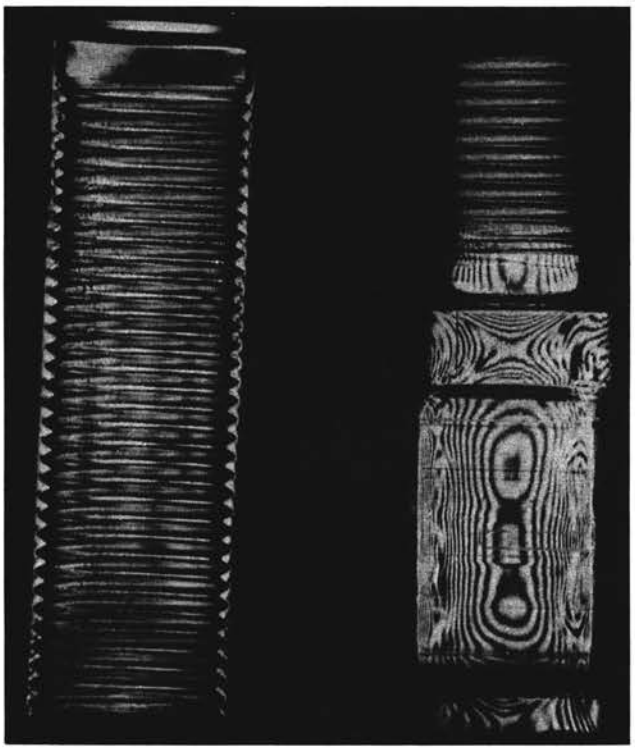

rate was approximately 2 °F per hour. A plot of the cooling curve for the annealing process is shown in Figure 10.

After the annealing was completed, the model was removed from the oven and examined in the polariscope to determine the effectiveness of the annealing process. The halowax bath was again used to view the three-dimensional model. The annealed model is shown in Plate VI. The elimination of the fringe pattern indicated that the annealing process was successful.

Stress Freezing

The model was assembled and each pin was tightened with 367 in-lb of torque. The model was placed in the loading frame previously installed in the oven as shown in Plate III. A load of seven pounds was applied to the model. This load was one pound less than the minimum load that would cause separation of the pin shoulder and the coupling after the 367 in-lb torque was applied. Inspection revealed the joint surface between the pin shoulder and the coupling remained in contact after the application of the seven-pound load.

The oven was heated to 270 °F, the critical temperature of Hysol 6000-OP, and maintained at this temperature until the thermocouple reading indicated sufficient time had elapsed for the entire model to be in thermal equilibrium. The oven was forced to cool at a constant rate by the mechanism shown in Plate III. The cooling rate was approximately 2 °F per hour. A plot of the cooling curve for the stress-freezing process is shown in Figure 11. The static load was maintained on the specimen until the specimen returned to room temperature.

PLATE VI

API STANDARD PIN AFTER ANNEALING

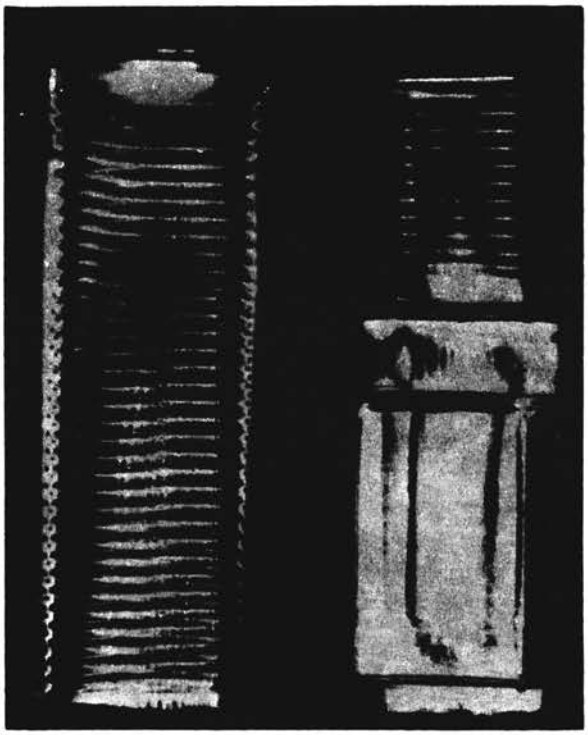

Slicing

The slices were cut from the sucker-rod joint by a milling machine in the manner indicated in Figure 1. The slicing was done at the Research and Development Laboratory, Oklahoma State University.

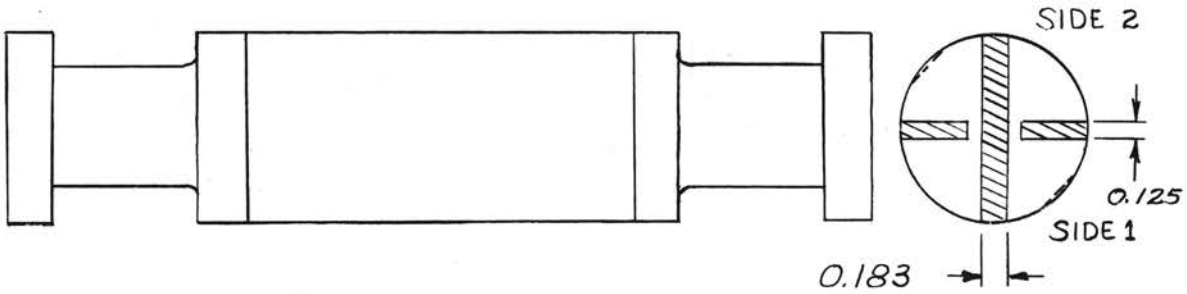

Figure 4. Orientation of Slices

The table feed rate was one-half inch per minute. The speed of the cutter was 190 revolutions per minute.

The slices were centered on diametral planes of the joint. The orientation of the slices was chosen such that the small flats on the coupling would not appear on the slice.

Examining and Photographing

The slices were supported in the halowax bath in such a manner that no extraneous fringes were introduced into the specimen. The halowax oil would not have been necessary if the customary procedure of sanding and rouge polishing had been practiced. The sanding and rouge-polishing technique was not used because of the possibility of rounding the edges of the slices. This would distort the true boundary pattern.

The quarter-wave plates were inserted into the polariscope in order to view the fringe pattern without the isoclinics. Due to the small number of fringes present, more accurate results were obtained by using the white light and counting the fringes by the technique of color matching. Color matching is an accepted method for determining the fringe order at a point when only a small number of fringes are present. In a stress pattern with a large number of fringes, the colors are close together and difficult to distinguish.

The polariscope was arranged for photographing the fringes in the model as shown in Plate IV. Monochromatic light was used to take the photographs, and the photographic procedure is described in Appendix A. The photographs were taken with the slices in a plane perpendicular to the optical path.

The fringe pattern for the center slice of the coupling shown in Plate VIII indicated that contact was maintained between the coupling and the shoulder of the pin during the stress-freezing operation. The fringe pattern in the threads of the undercut pin and the standard API pin is shown in Plate IX. The threads were on side one of the center slice and, therefore, experienced similar loading conditions.

CHAPTER V

RESULTS

The fringe pattern of the standard API pin before the slicing operation is shown in Plate VII. The symmetry of the fringe pattern indicates that an axial load was present on the model during the stress-freezing operation.

The loading condition resulted in a maximum of three fringes being present in the center slice of the model. The fringe order at the root of each thread was determined by the technique of color matching.

The material color value, which is equal to the material fringe value, is the difference in principal stresses required to produce one fringe in a specimen that is one-inch thick. The model color value is the difference in principal stresses required to produce one fringe in the model. The material fringe value g and the model fringe value G are related by

$$Gt = g$$

where t is the thickness of the model; thus,

$$G = \frac{1.35}{0.183} = 7.377 \text{ psi/fringe}.$$

The number of fringes in the model may be expressed as

$$N = \frac{P-Q}{G}.$$

The principal stress Q at the root of the thread was zero since this point was a free boundary; only one principal stress can exist at

PLATE VII

API STANDARD PIN WITH FROZEN STRESS

PATTERN BEFORE SLICING

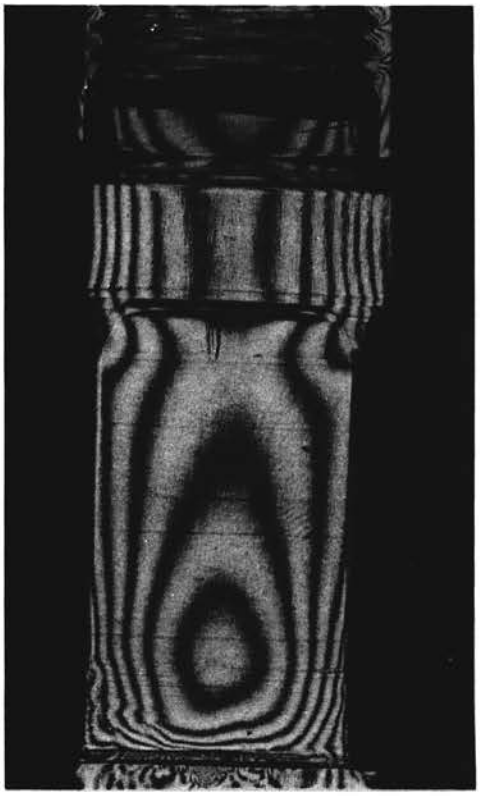

a free boundary. The principal stress P may be expressed as

$$P = GN$$

$$P = 7.377\,(N)\ \text{psi}$$

where N is the fringe order (N = 1 for the first green fringe).

The stress value of the first yellow equals one third of the stress of the first green and similarly that of the first red equals two thirds that of the first green. Likewise, the second yellow equals four thirds of the first green; the second red, five thirds of the first green; etc. (7). The stress at the root of each thread for the API standard pin is shown in Table II. The stress at the root of each thread for the undercut pin is shown in Table III. The fringe pattern at the root of the threads for both pins is shown in Plate IX.

TABLE II

MAXIMUM STRESS VALUES AT THE ROOTS OF

THE STANDARD API PIN

Distance from First Root at the Free End of the Pin	Fringe Order		Stress	
	Side 1	Side 2	Side 1	Side 2
inches			psi	psi
0	1G	1G	7.38	7.38
0.1	1G	2R	7.38	12.29
0.2	1G	2R	7.38	12.29
0.3	1G	1G	7.38	7.38
0.4	1G	2G	7.38	14.75
0.5	1G	2G	7.38	14.75
0.6	2G	2G	14.75	14.75
0.7	2G	2G	14.75	14.75
0.8	2R	2R	12.29	12.29
0.9	2R	3G	12.29	22.12
1.0	2Y	2G	9.83	14.75
1.1	2Y	2R	9.83	12.29
1.2	2Y	1G	9.83	7.38

TABLE III

MAXIMUM STRESS VALUES AT THE ROOTS OF

THE UNDERCUT PIN

Distance from First Root at the Free End of the Pin	Fringe Order		Stress	
	Side 1	Side 2	Side 1	Side 2
inches			psi	psi
0	1G	1G	7.38	7.38
0.1	2G	2G	14.75	7.38
0.2	2G	1G	14.75	7.38
0.3	2G	2G	14.75	14.75
0.4	2G	2G	14.75	14.75
0.5	3G	2G	19.6	14.75
0.6	3R	3G	19.6	22.1
0.7	3R	3R	19.6	19.6
0.8	2R	3R	12.29	19.6
0.9	2R	2G	12.29	14.75
1.0	2R	3Y	12.29	17.2
1.1	2R	3Y	12.29	17.2
1.2	2R	3Y	12.29	17.2
1.3	2G	2G	14.75	14.75
1.4	2R	2Y	12.29	9.83

CHAPTER VI

ANALYSIS OF RESULTS

The fringe patterns on the end of the coupling slices indicated that the contact pressure was not uniform around the circumference of the coupling. This probably was the result of the end of the coupling not being in a plane perpendicular to the axis of the threads. The higher stress on side two of the center slice indicated that the uneven distribution of the contact pressure may have subjected the pins to a small amount of bending.

The fringe patterns at the ends of the coupling slices, other than the one shown in Plate VIII, indicated that small contact pressures existed between the shoulders of the pins and the coupling. As the contact pressure between the shoulder of the pin and the coupling approaches zero, the load distribution among the threads on the pin approaches the load distribution which exists among the threads of a stud in a threaded hole. Since the load distribution among the threads of a stud is more uniform than among the threads of a bolt and nut combination, the undercut portion of the pin would appear to have little effect on the load distribution among the threads when the contact pressure between the shoulder of the pin and the coupling is small.

The low contact pressure present in the model that was tested would account for some similarity of the load distribution in the two pins. When a low contact pressure is involved, the undercut pin would experience

PLATE VIII

CENTER SLICE OF COUPLING

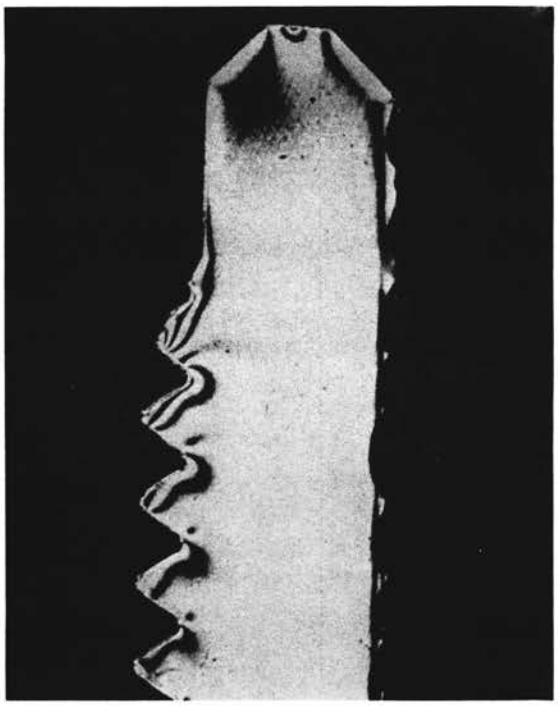

PLATE IX

CENTER SLICE FRINGE PATTERN

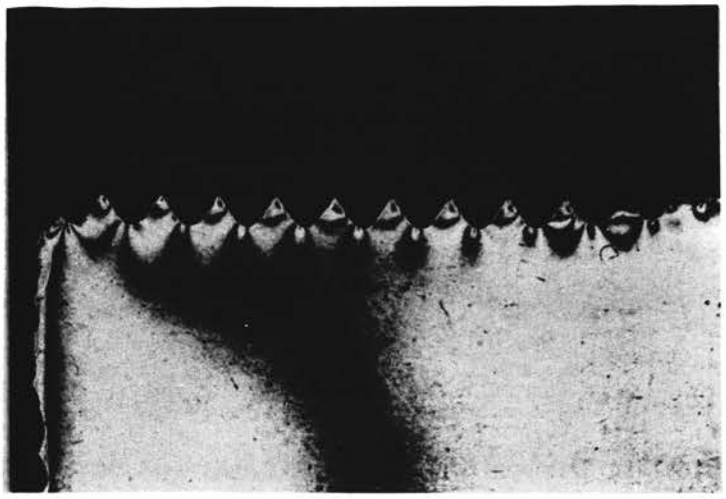

1. Standard API Pin

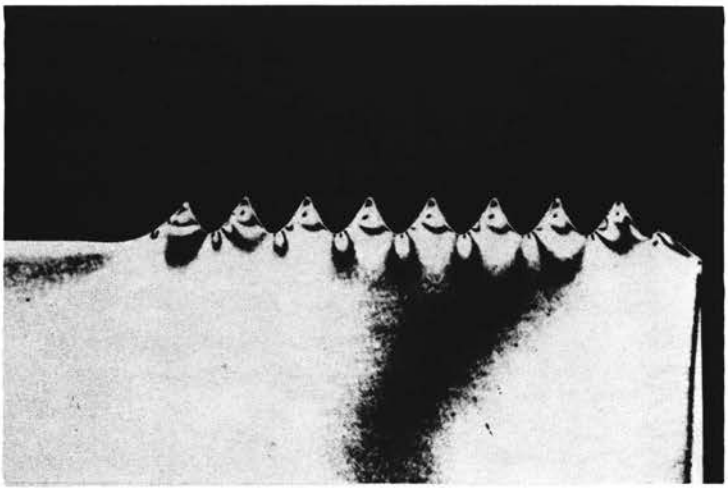

2. Undercut Pin

a higher stress because it has a fewer number of threads.

The maximum stress value at the root of each thread was expressed as a multiple of the experimental stress of 7.377 psi at the center of the pin. Each fringe indicated a difference of principal stresses. However, one of the principal stresses was zero at the root of the thread and the center of the pin. Therefore, the principal stress was directly proportional to the fringe order at these points. The stress ratio for each thread is shown in Table IV and Figures 5, 6, 7, and 8.

TABLE IV

FILLET STRESS VALUES EXPRESSED AS MULTIPLES OF

THE AVERAGE STRESS IN THE PIN

Distance from First Root at the Free End of the Pin in inches	Standard API Pin k*		Undercut Pin k*	
	Side 1	Side 2	Side 1	Side 2
0	1.0	1.0	1.0	1.0
0.1	1.0	1.6	2.0	1.0
0.2	1.0	1.6	2.0	1.0
0.3	1.0	1.0	2.0	2.0
0.4	1.0	2.0	2.0	2.0
0.5	1.0	2.0	2.6	2.0
0.6	2.0	2.0	2.6	3.0
0.7	2.0	2.0	2.6	2.6
0.8	1.6	1.6	1.6	2.6
0.9	1.6	3.0	1.6	2.0
1.0	1.3	2.0	1.6	3.3
1.1	1.3	1.6	1.6	3.3
1.2	1.3	1.0	1.6	3.3
1.3	---	---	2.0	2.0
1.4	---	---	1.6	1.3

*$k = \frac{\text{Maximum Fillet Stress}}{\text{Average Stress}}$

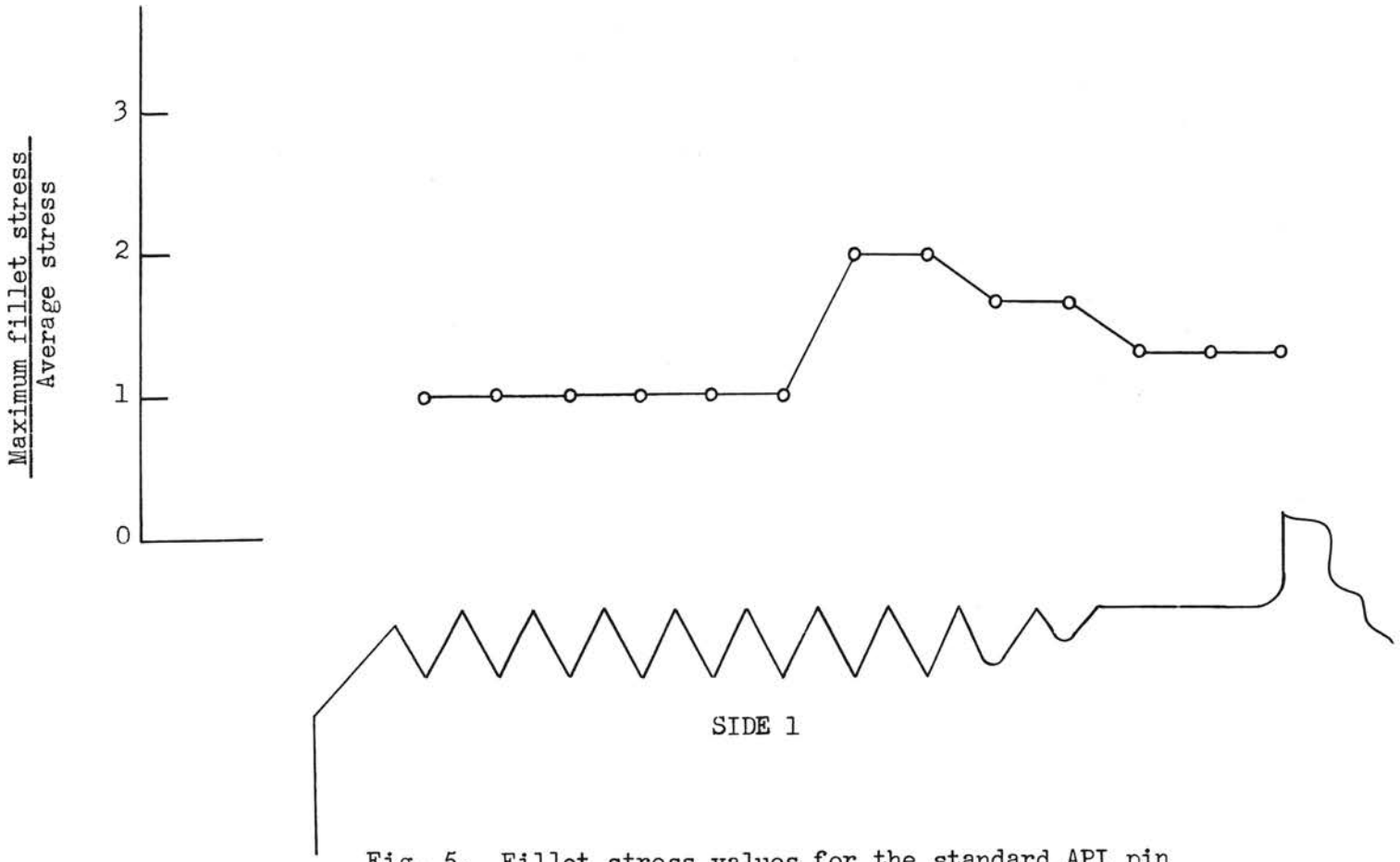

Fig. 5. Fillet stress values for the standard API pin

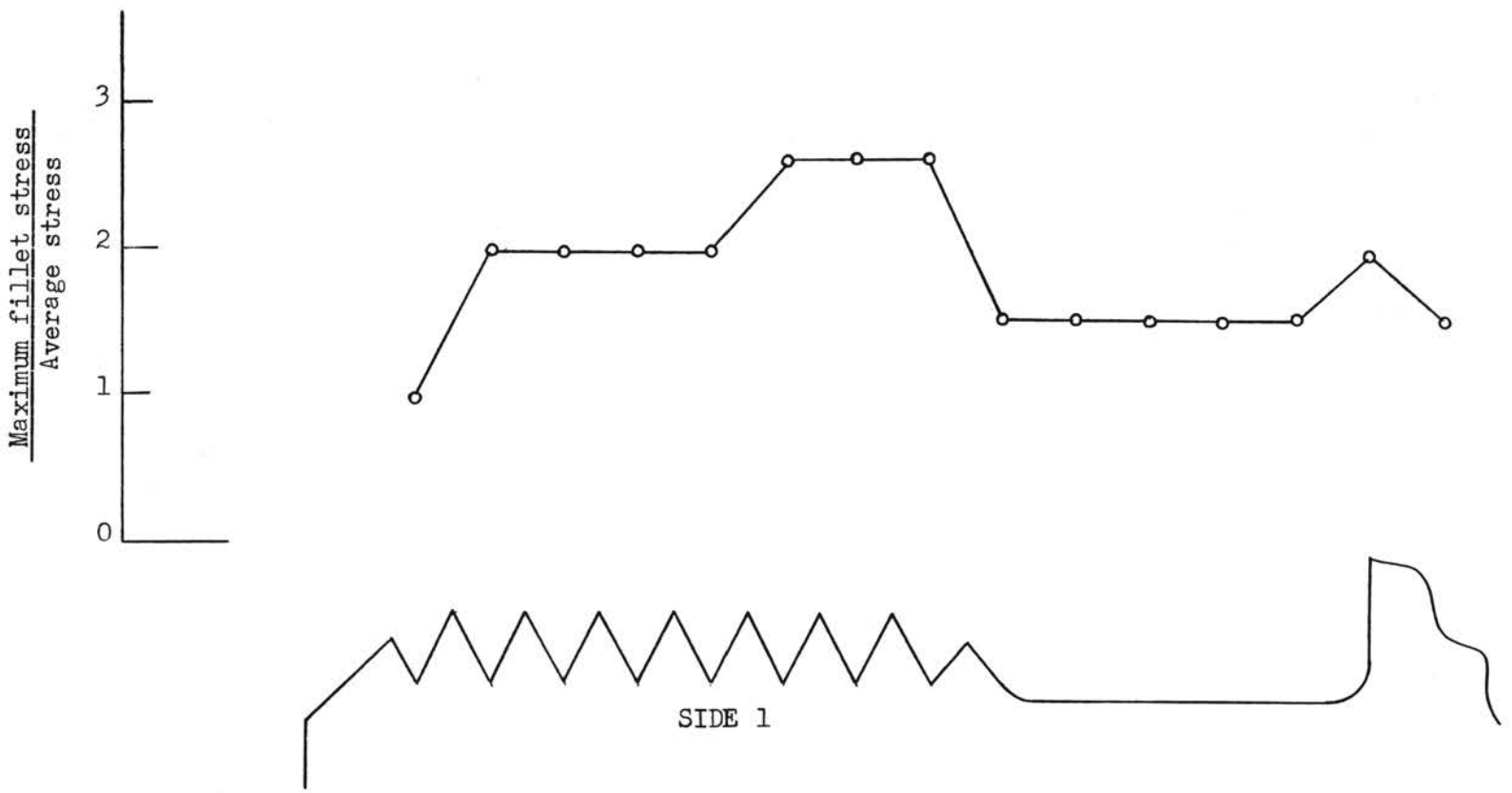

Fig. 6. Fillet stress values for the undercut pin

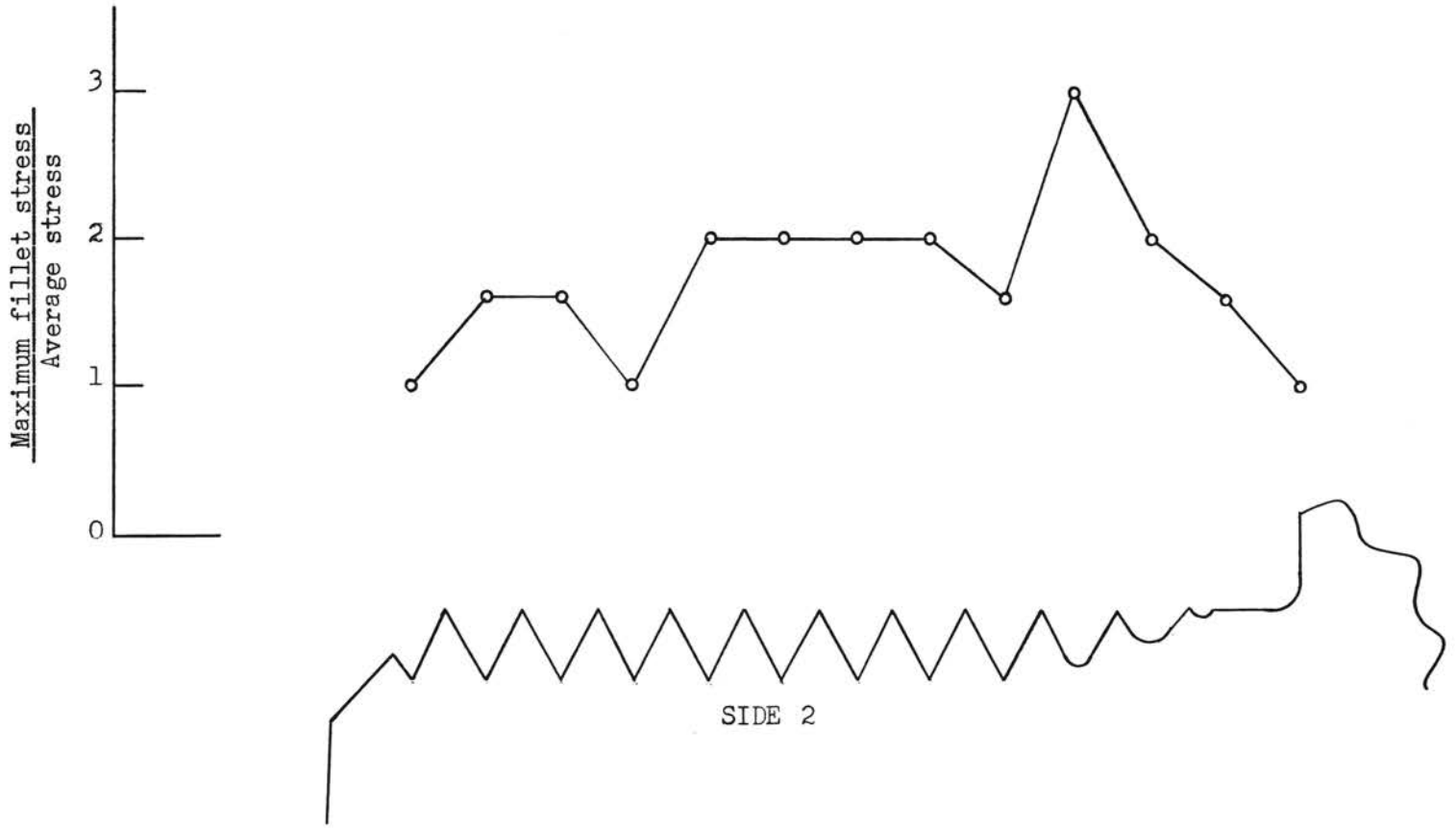

Fig. 7. Fillet stress values for the standard API pin

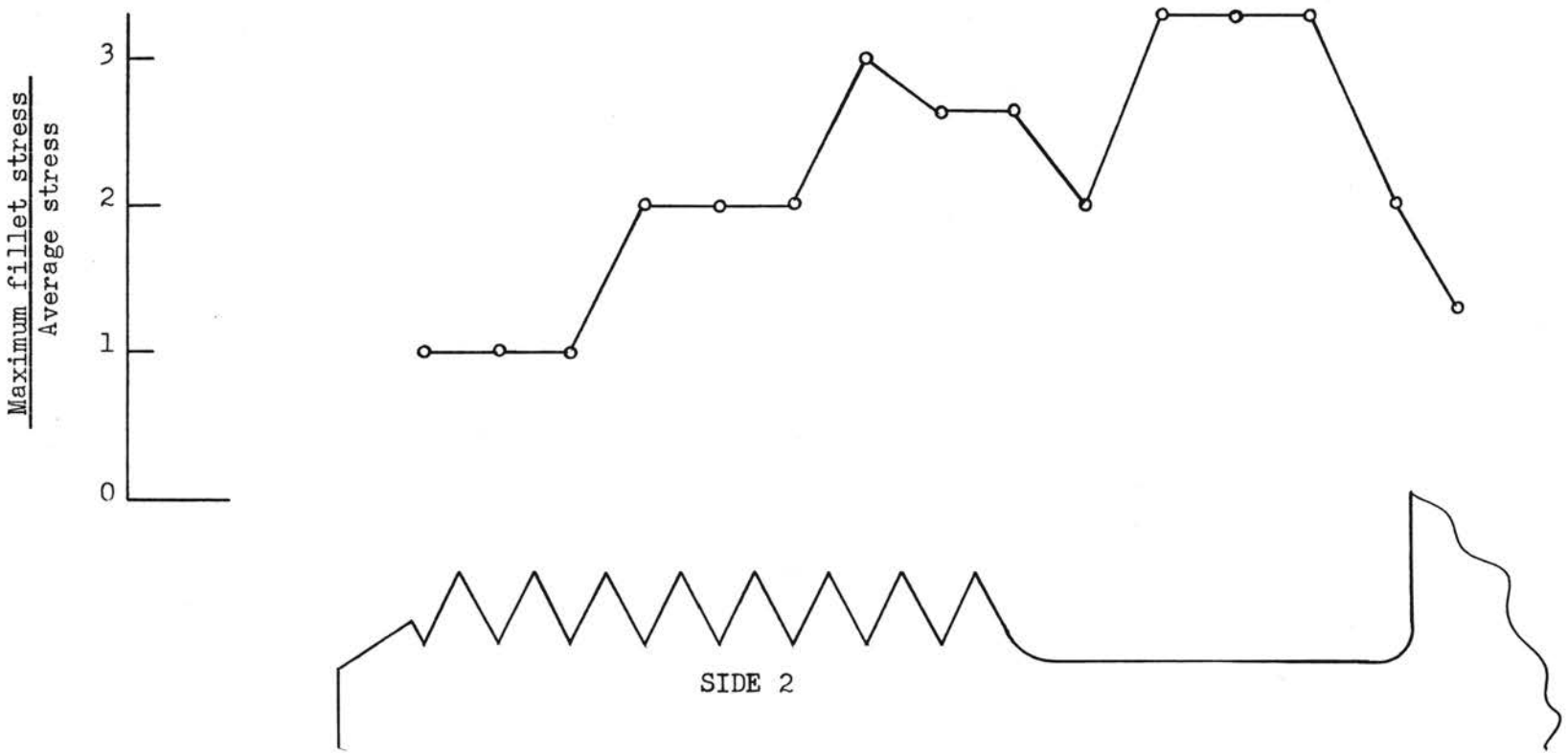

Fig. 8. Fillet stress values for the undercut pin

CHAPTER VII

CONCLUSIONS AND RECOMMENDATIONS

The purpose of this research was to compare the stress concentration in two types of sucker-rod pins.

The maximum stress concentration was observed at the first full thread on each pin. The stress concentration in the pins was less than the stress concentration for a conventional bolt and nut design. The smaller stress concentration in the pins is a result of the combination of the preloading of the pins and the tension on the coupling of the sucker-rod joint.

The undercut pin experienced a higher stress concentration than the standard API pin. This appeared to be the result of a fewer number of threads on the undercut pin.

There appeared to be some bending in the pin due to an uneven contact pressure between the shoulder of the pin and the collar. This may have been a result of the failure to machine the end of the coupling. The bending appeared to produce a larger stress concentration in the undercut pin. Bending should not occur in a sucker-rod pin; however, it often does.

The fringe pattern indicated that the undercut pin experienced a maximum uniform stress over a greater length of the pin. This is a recognized advantage in absorbing energy loads.

The conclusion concerning the experimental technique was that more accurate results could have been obtained by the use of a larger load on the model. More accurate results could be obtained by repeating the test and incorporating the following recommendations.

A satisfactory lubricant for the threads would allow for a larger preload of the pins. A larger external load could be used with a larger preload, and contact between the shoulder of the pin and the coupling could be maintained.

One of the criteria for selection of the lubricant would be that it not affect the optical or physical properties of the Hysol 6000-OP during the stress-freezing operation.

The bending present in the pins could have been introduced as a result of irregular fitting of the square corners of the wrench flats to the loading frame.

It would be an advantage to use a circular holding section with close tolerances.

The stress pattern at the threads was affected because of the chipping of the threads during the slicing of the model. Some changes in the slicing operation would be desirable.

Additional fringes could also be produced by a thicker center slice. A thicker slice would not be desirable unless the over-all size of the model was increased because the principal stresses are in diametral planes and a thicker slice would not have a uniform difference in principal stresses across its width.

Additional fringes could have also been obtained from the center slices of the model if a reflecting polariscope had been available.

The light contact pressure between the shoulder of the pin and the coupling resulted in a similar load distribution for each pin. In order to simulate the desirable operating conditions for the pin, the joint should be tightened until a considerable amount of compression will exist in part of the coupling when the external load is applied. An investigation should be conducted to obtain a comparison of the load distribution for different amounts of tightening.

SELECTED BIBLOGRAPHY

(1) Hardy, A. A., "Sucker-Rod Joint Failures," Drilling and Production Practice, 214-225, (1952).

(2) Hetenyi, M., "A Photoelastic Study of Bolt and Nut Fastenings," American Society of Mechanical Engineers Transactions, Vol. 65, A-93, (1943).

(3) Hardy, A. A., "Correcting Sucker-Rod Troubles As Seen by a Manufacturer." W.C. Norris Manufacturer Inc., Tulsa, Oklahoma.

(4) Spencer, M. M. "Three-Dimensional Photoelastic Analysis Of The Surface Stress Distribution In The Pin Of A Lap Joint," Doctor of Philosophy Thesis, Oklahoma State University, 1960.

(5) Hardy, A. A., "Undercut Pins and Rolled Threads For Sucker-Rods," W. C. Norris Manufacturer Inc., Tulsa, Oklahoma, (1961).

(6) Spotts, M. F., Design Of Machine Elements, (Prentice-Hall, Inc.: Englewood Cliffs, N. J., 1953).

(7) Frocht, M. M., Photoelasticity, (John Wiley and Sons: New York, 1949), I.

(8) Cerro Alloy Casting Procedures Manual. 300 Park Avenue, New York 22, New York: Cerro De Pasco Sales Corporation.

APPENDIX A

PHOTOGRAPHIC PROCEDURES

A permanent record of the test was obtained by photographing the fringe pattern in the model. The correct exposure time for the photograph was determined by making a few sample photographs. An f-stop setting of f-5.6 was used for focusing the camera because it allowed sufficient light to reach the ground-glass plate of the camera. The camera was carefully focused so that a distinct image appeared on the ground-glass plate. The exposure time was estimated to be two seconds. To determine the correct exposure time more accurately, exposures were obtained for times both less and greater than two seconds. Four successive exposures were made for one second, three seconds, five seconds, and fifteen seconds respectively. The three-second exposure and f-5.6 setting produced good results. This combination was used for all of the fringe pattern photographs in this investigation.

The films were developed immediately after exposure to insure that a good negative had been obtained. Kodak Super Panchro-Press Type B film must be developed in a totally dark room. Three trays containing the developer, the stop bath, and the acid fixer were used for the developing process. The average developing time for Dk-60-a developer was approximately four minutes at 70 ^{o}F.

After the negative was removed from the developer, it was rinsed in plain water. Plain water may be substituted for a stop bath in the

development process. The developer should be rinsed from the negative to increase the useful life of the fixing bath. The negative was agitated in the water for approximately fifteen seconds.

Once the development process was completed, it was necessary to remove the unexposed and undeveloped silver bromide by means of a hypo solution. This process is known as fixation. After rinsing the negative in the stop bath or plain water, it was placed in the acid fixer and allowed to remain for ten minutes. The fixing bath may be used repeatedly; however, when the time taken to clear the film exceeds ten minutes, the solution should be discarded.

The practice of using two fixing baths in succession is recommended. Negatives are transferred from the first bath to the second bath in five-minutes time, whether the negatives are clear or not. When the first bath becomes very slow in action or cloudy, it is discarded or replaced by the second bath--a fresh one taking the place of the second bath. This plan insures more rapid fixation.

The negative could be exposed to white light as soon as the developer retained in the film has been neutralized. It was safe to expose the negatives to light after approximately two minutes in the fixer solution. After the fixation process was completed, the negatives were washed in plain water in the washing tub for approximately thirty minutes in order to completely remove the developing and fixing solutions.

The negatives were taken from the washing bath to the drying chamber. Before placing the negatives in their drying position, the surface moisture was removed from the negatives in order to eliminate drying marks on the print.

Prints of the negatives were made in order to eliminate excessive handling of the negatives during the analysis of the problem. The prints were exposed on a contact printer actuated by a Lektra Laboratories, Inc., Model TM-8 timer, which was set for 0.3 seconds.

The prints were developed under a safe light for approximately 45 seconds in Vividol print developer. The washing and fixing processes for the prints were the same as for the film.

Glossy prints were obtained by use of the Pako Electrogloss photo dryer.

The photographic materials used in this investigation were as follows:

1. Kodak Super Panchro-Press Type B film
2. Kodak Dk-60-a developer

   The average development time for film is four minutes in a tray or five minutes in a tank with the Dk-60-a developer at 70 °F.
3. Anscro Vividol print developer

   The average development time for paper is 45 seconds to one minute at 68 °F.
4. Kodak acid fixer

   The negatives require approximately ten minutes in fresh fixer at 65-70 °F.

APPENDIX B

CASTING PROCEDURE

The model was cast in Cerrobend for the cutting operation. Cerrobend is an alloy with a low melting temperature that expands when it solidifies; thus, it is a good support for the model during the slicing operation. The characteristic of expansion and low melting temperature was the major reason for selecting Cerrobend as the casting material.

In order to eliminate excessive heating of the model, a minimum amount of Cerrobend was used. Cerrobend is a poor conductor of heat and therefore cools slowly. In order to remove the heat rapidly, the mold was chilled immediately after casting. The mold was chilled by wiping with cold water and by directing a stream of air across the casting.

The procedure for mold preparation is described in Cerro Alloy Casting Procedures. (8).

APPENDIX C

PROPERTIES OF CERROBEND

TABLE V

PHYSICAL PROPERTIES OF CERROBEND

Melting Temperature	158 ^{o}F
Density	0.339 lb/in^3
Tensile Strength	5990 lb/in^2
Latent Heat of Fusion	14 BTU/lb

APPENDIX D

PROPERTIES OF HYSOL 6000-OP

TABLE VI

PHOTOELASTIC PROPERTIES OF HYSOL 6000-OP

Fringe Value at 270 °F (tensile)	1.35 psi/fr/in
Fringe Value at 77 °F (tensile)	57 psi/fr/in
Stress Freezing or Critical Temperature	270 °F
Annealing Temperature	280 °F
Annealing Cooling Rate	no greater than 2 °F/hr
Poisson's Ratio	0.500
Figure of Merit at 77 °F (Q = Eeff/feff)*	7250
Figure of Merit at 270 °F	1620

*Eeff Modulus of Elasticity
feff Fringe value in frozen stress test

TABLE VII

MECHANICAL PROPERTIES OF HYSOL 6000-OP

	77 °F	270 °F
Modulus of Elasticity, psi	480,000	2,190
Refractive Index	1.605	
Tensile Strength, psi	12,000	3,540
Compressive Strength, psi	18,000	
Flexural Strength, psi	18,500	
Thermal Coefficient of Expansion, Linear/°C . .	4.7×10^{-5}	8.2×10^{-5}

APPENDIX E

LOADING FRAME DETAILS

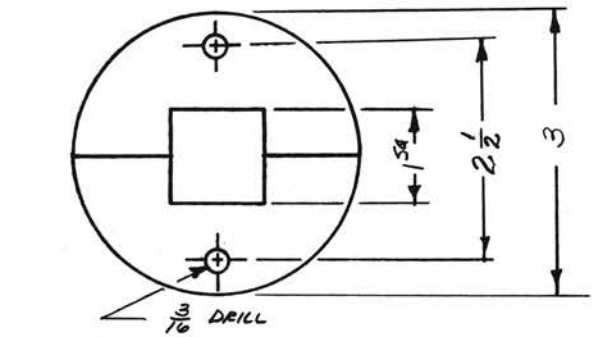

LOWER PIN CLAMP

1 - REQ'D 1/4 MILD STEEL PLATE

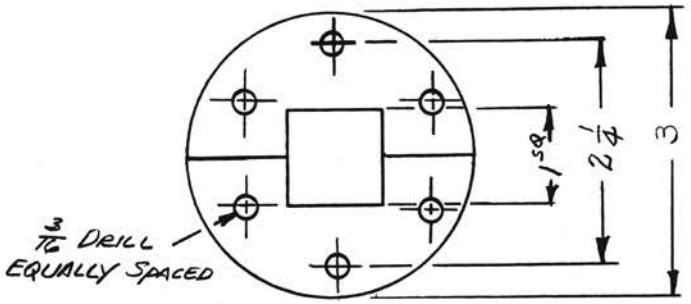

UPPER PIN CLAMP

1 - REQ'D 1/4 MILD STEEL PLATE

SCALE 1/2 = 1

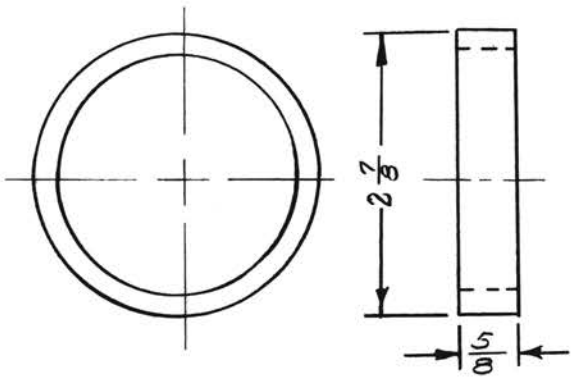

UPPER PIN CLAMP SPACER

1 REQ'D MILD STEEL

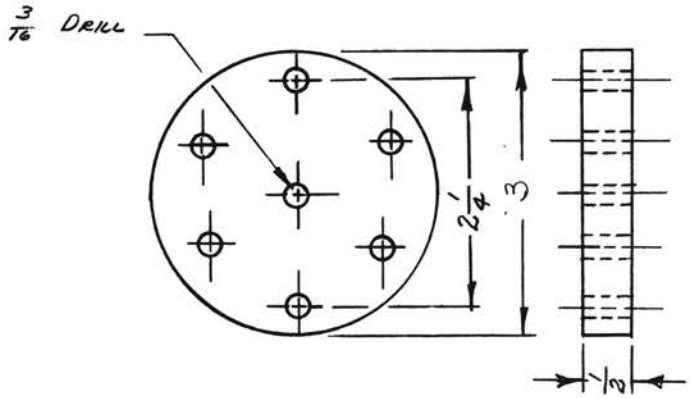

LOADING PLATE

1 - REQ'D 1/2 MILD STEEL PLATE

Figure 9a. Details of Loading Frame Components, Sheet 1 of 3

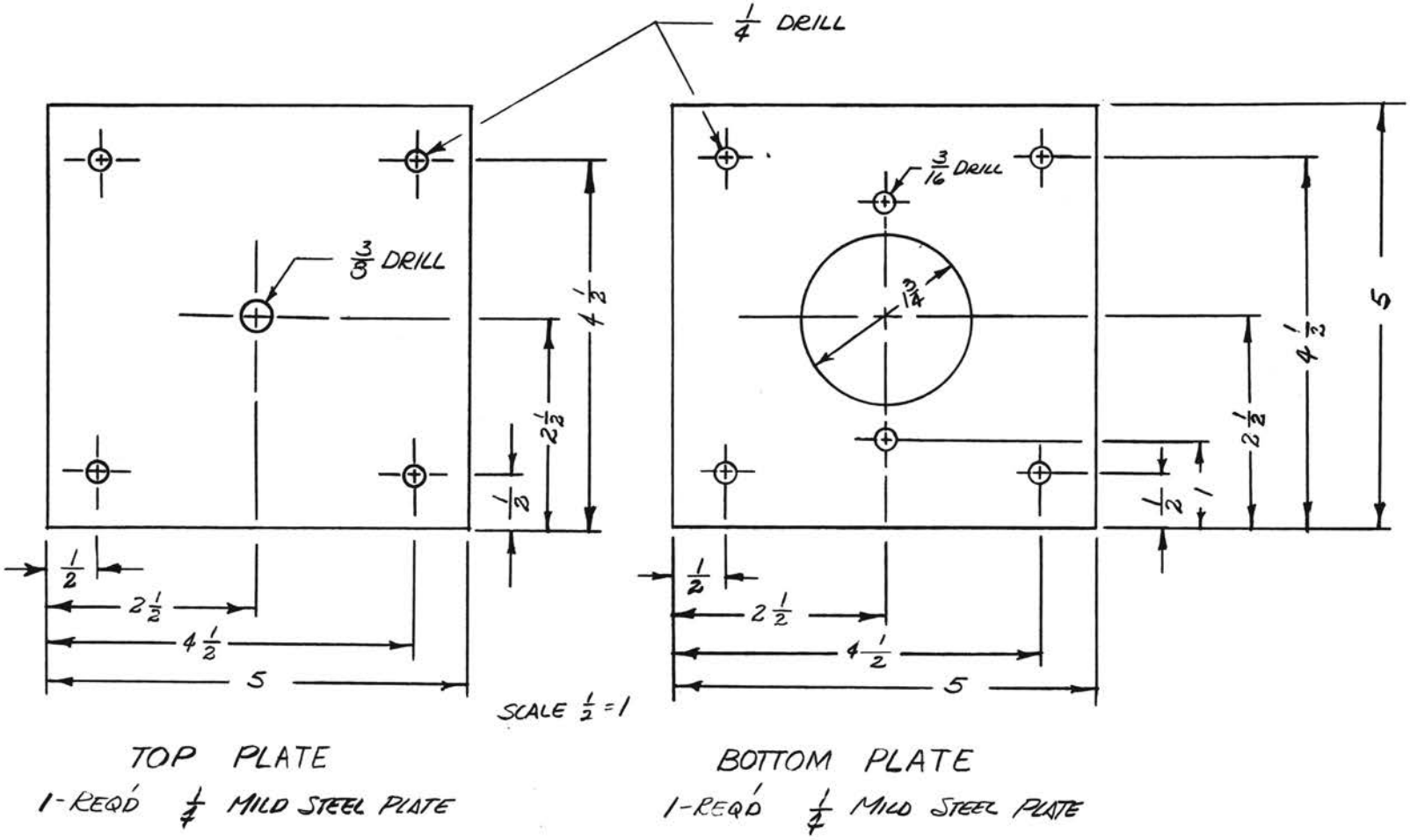

Figure 9b. Details of Loading Frame Components, Sheet 2 of 3

ADDITIONAL LOADING FRAME COMPONENTS

Sheet 3 of 3

1/2 INCH DIAMETER STEEL PIPE, 11 INCHES LONG, 4 REQUIRED

1/4 INCH DIAMETER THREADED ROD, 13INCHES LONG, 4 REQUIRED

5/32 x 1 1/2 INCH BRASS MACHINE SCREWS, 8 REQUIRED

1/16 INCH DIAMETER AIRCRAFT CONTROL CABLE, 4 FEET REQUIRED

1 INCH DIAMETER PULLEYS, 2 REQUIRED

APPENDIX F

OVEN CONTROLS

TABLE VIII

ANNEALING OVEN CONTROL

Voltage (Volts)	Oven Temp. (°F)	Room Temp. (°F)
28	280	80
24	279 - 270	75
22	269 - 260	77
20	259 - 240	73
18	239 - 220	70
16	219 - 208	74
14	207 - 188	74
12	187 - 166	74
10	165 - 136	78
off	135 -	

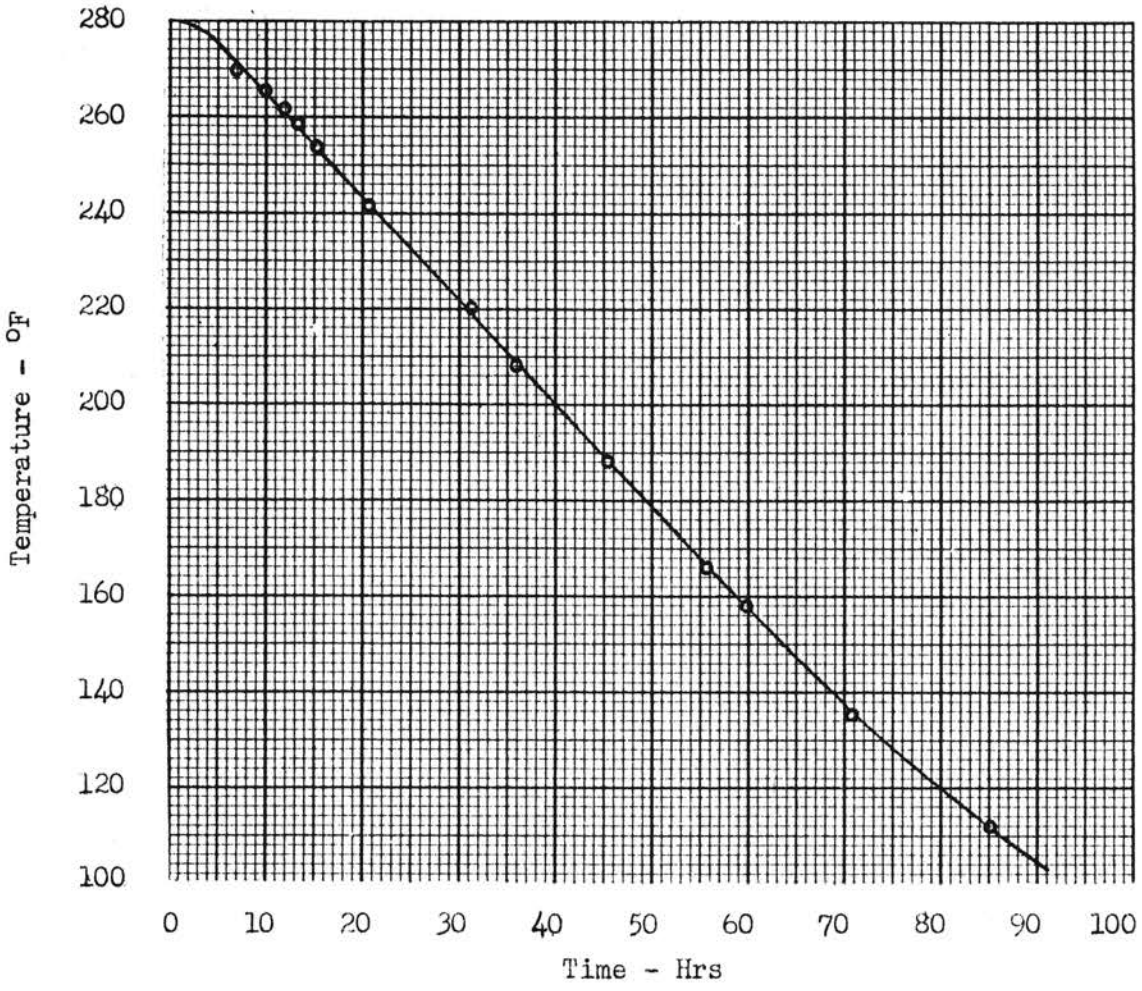

Figure 10. Annealing Oven Cooling Rate

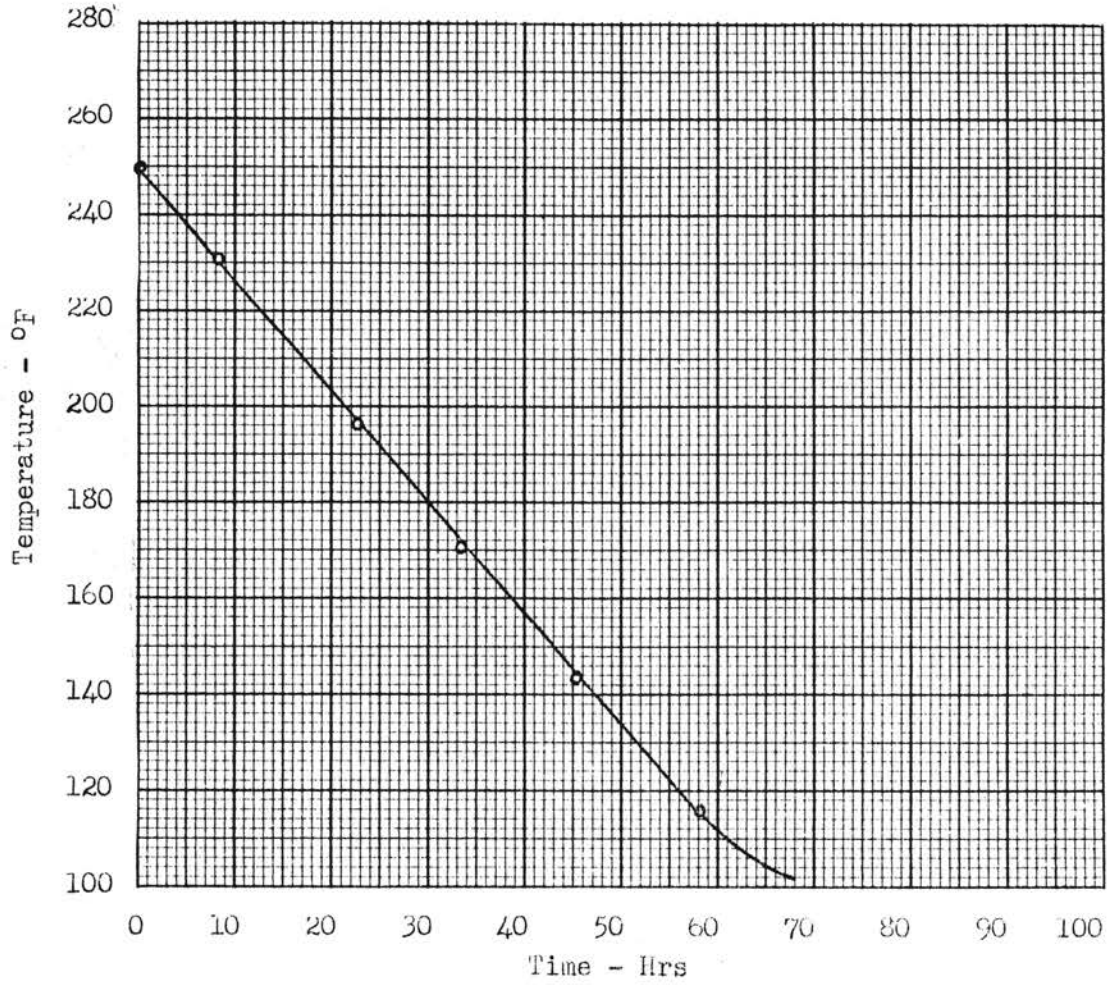

Figure 11. Stress-Freezing Oven Cooling Rate

VITA

Monroe Upton Ayres, Jr.

Candidate for the Degree of

Master of Science

Thesis: THREE-DIMENSIONAL PHOTOELASTIC ANALYSIS OF THE LOAD DISTRIBUTION IN A SUCKER-ROD JOINT

Major Field: Mechanical Engineering

Biographical:

Personal Data: Born at Madill, Oklahoma, July 4, 1937, the son of Monroe U. and Martha J. Ayres.

Education: Attended grade school in Madill, Oklahoma; graduated from Madill High School in 1955; received the Bachelor of Science degree from the Oklahoma State University, with a major in Mechanical Engineering, in January, 1960; completed the requirements for the Master of Science degree in May, 1961.

Experience: Employed as an assistant welder for National Tank Company during the summers of 1956 and 1957 in Tulsa, Oklahoma; employed as a student assistant for the School of Mechanical Engineering at Oklahoma State University during 1958-1960; employed as a full-time instructor for the School of Mechanical Engineering at Oklahoma State University from January, 1960, to May, 1961, instructing courses in Mechanical Drawing, Machine Drawing, Kinematics, and Machine Design.

Honorary Organizations: Pi Tau Sigma; Sigma Tau; Blue Key.

Honors and Awards: Who's Who in American Colleges and Universities, 1960; St. Pat Salutes Award, 1960; O.S.U. Redskin Congratulate, 1959; College of Engineering Student Senator, 1959; Hughes Tool Company Scholarship, 1960.